SPECTRAL INTERPOLATION OF AEROSOL EXTINCTION COEFFICIENTS

Ghislain Franssens, Didier Fussen, Martine De Mazière, Dominique Fonteyn, and Quentin Errera

Belgian Institute for Space Aeronomy
Ringlaan 3, B-1180 Brussels, BELGIUM
E-mail: ghislain.franssens@oma.be

ABSTRACT

A new approach to the problem of spectral interpolation of aerosol extinction coefficients is presented. The proposed algorithm is applicable to non-absorbing, spherical particles and is based on the Anomalous Diffraction Approximation (ADA). The interpolant consists of a linear combination of carefully designed basis functions, each possessing the correct spectral behaviour of an extinction function. The expansion coefficients are obtained by minimising a fitting cost function, using a Generalized Reduced Gradient Method (GRGM), with constraints.
The performance of the algorithm has been examined when applied to sparse data, corrupted by errors. The usefulness of the algorithm in solving the spectral inverse problem, i.e. in deriving the aerosol size distribution from the extinction coefficient, is discussed. A number of numerical test examples are shown.

1. INTRODUCTION

Measurements of the optical extinction coefficient β [1/m] are typically performed at a limited number of discrete wavelengths or in limited, densely sampled bands.
For certain applications, one needs to know β also at wavelengths where no measurements were made. An example is the retrieval of the concentration of an atmospheric trace constituent from total optical extinction, measured at a particular wavelength. To find the contribution from the constituent alone, one must subtract the aerosol component at that wavelength (e.g. O_3 at 0.6 μm).
Another application is the retrieval of derived aerosol parameters, which requires the knowledge of $\beta(\lambda)$ over a broad range (UV to the far IR) [Refs. 1-2]. An example is the aerosol number density distribution $N(r)$ [1/m^4], obtained from the spectral inversion of the extinction coefficient.
Spectral interpolation and this spectral inversion are closely related. On one hand, experimental data requires interpolation or fitting before spectral inversion can be carried out. On the other hand, the spectral interpolation problem becomes trivial, once the underlying aerosol number density is known. In the approach presented here, we consider the problems of interpolation and inversion together.
General light scattering and absorption is described by Mie theory and is mathematically complex [Ref. 9]. A convenient approximation to Mie scattering theory is the Anomalous Diffraction Approximation (ADA). It is valid for spherical particles, with radius r and (complex) refractive index $m = n - in'$, when $|n-1| << 1 << kr$, $k = 2\pi/\lambda$. The ADA is sufficiently accurate for most practical purposes and is mathematically more tractable. It incorporates both the Rayleigh limit for small r (extinction efficiency tends to zero) and the geometrical-optics limit for large r (extinction efficiency tends to 2), and therefore possesses the major features of light scattering by spherical particles larger than the wavelength.
A number of interpolation and inversion methods have been presented in the literature before [Refs. 3-8]. In this paper we present some first results obtained by a new algorithm for spectral interpolation. As a by-product, we also get an approximation for the underlying aerosol number density distribution. We focus attention on the practical case where $\beta(\lambda)$ is measured at only a limited number of wavelengths and the data is corrupted by experimental and/or processing errors [Ref. 8].
We begin with a brief summary of spectral inversion theory and present an explicit analytical inversion formula. Based on this formula, we propose a discrete set of basis functions, and represent the spectral interpolation function as a linear combination of these basis functions. The interpolation function is then fitted to the given data, by minimising a cost function, using a Generalized Reduced Gradient Method (GRGM), with constraints [Refs. 11-12]. Finally, expressions are given to compute the aerosol total number density, total surface density and total volume density, (assuming spherical particles).
Our method was tested on simulated data for single and bimodal distributions, using ADA as forward model, and for non-absorbing, non-dispersive particles (i.e. having a real and constant refractive index). The noise tolerance of the algorithm and the accuracy of the interpolation were examined, and this is illustrated by a number of examples.
This work is still in progress and efforts are underway to also incorporate absorption and dispersion effects in the algorithm.

2. THEORY

For our theoretical framework we use the ADA, applied to non-absorbing, non-dispersive, spherical aerosol particles. That is, the refractive index n of the particles is assumed to be real and independent of the wavelength. The extinction efficiency $Q_{eff}(2\kappa r)$, where $\kappa = (n-1)k$ is the effective wavenumber, is given by [Ref. 9]

$$Q_{eff}(2\kappa r) = 2 - 4\frac{\sin(2\kappa r)}{2\kappa r} + 4\frac{1-\cos(2\kappa r)}{(2\kappa r)^2} \qquad (1)$$

valid when $\kappa r >> |n-1|$.
The relation between the aerosol extinction function $\beta(\kappa)$ and the aerosol number density distribution $N(r)$ is

$$\beta(\kappa) = \int_0^{+\infty} \pi r^2 Q_{eff}(2\kappa r) N(r) dr \qquad (2)$$

It is mathematically more convenient to use the effective wavenumber κ instead of the wavelength as independent variable and to work with a modified extinction function $B(\kappa)$, instead of the function $\beta(\kappa)$. Eq. (2) is rewritten as

$$B(\kappa) = \int_0^{+\infty} K(\kappa, r) S(r) dr \tag{3}$$

with

$$B(\kappa) \overset{\Delta}{=} b_\infty - b(\kappa),\ b(\kappa) \overset{\Delta}{=} 2\beta(\kappa) \tag{4a}$$

$$b_\infty \overset{\Delta}{=} \lim_{\kappa \to +\infty} b(\kappa) = \int_0^{+\infty} S(r) dr \overset{\Delta}{=} S_{tot} \tag{4b}$$

$$\begin{aligned} K(\kappa, r) &\overset{\Delta}{=} \frac{1}{2}\left(2 - Q_{eff}(2\kappa r)\right) \\ &= 2\left(\frac{\sin(2\kappa r)}{2\kappa r} - \frac{1-\cos(2\kappa r)}{(2\kappa r)^2}\right) \end{aligned} \tag{4c}$$

$$S(r) \overset{\Delta}{=} 4\pi r^2 N(r) \tag{4d}$$

The quantity (4d) is the aerosol surface density distribution, in [1/m^2]. Eq. (3) is a Fredholm integral equation of the first kind, with symmetric kernel $K(\kappa, r)$, over the domain $R^+ \times R^+$. In [Ref. 10] it is proved that (3) has the explicit inverse

$$S(r) = \frac{4}{\pi} \int_0^{+\infty} (\kappa r)^2 K(\kappa, r) B(\kappa) d\kappa \tag{5}$$

and that this inverse is unique.

The inversion formula is mainly of theoretical importance and served as a basis for the construction of a more practical algorithm. Due to the oscillatory behaviour of the inverse kernel, this formula will be of little use, when only a few spectral measurements are available. For these more difficult cases we now introduce a more practical algorithm.

Consider an ordered sampling of the r-axis, $\{r_n,\ n = 0, N\}$ and define a set of discrete basis functions $\{B_n(\kappa),\ n = 1, N\}$, by

$$\begin{aligned} B_n(\kappa) &= \frac{2}{\sqrt{\pi}} \frac{r_n^c}{h_n} \kappa \int_{r_{n-1}}^{r_n} K(\kappa, r') dr' \\ &= \frac{2}{\sqrt{\pi}} \frac{r_n^c}{h_n} \left(\frac{1-\cos(2\kappa r_n)}{2\kappa r_n} - \frac{1-\cos(2\kappa r_{n-1})}{2\kappa r_{n-1}} \right) \end{aligned} \tag{6}$$

where

$$\begin{aligned} h_n &= r_n - r_{n-1} \\ r_n^c &= (r_n + r_{n-1})/2 \end{aligned} \tag{7}$$

The discrete basis functions are such that $\frac{B_n(\kappa)}{\kappa}$ is the extinction function of a block-like surface density distribution $S_n(r) = \frac{2}{\sqrt{\pi}} r_n^c \frac{\Pi(r - r_n^c; h_n)}{h_n}$.

The discrete basis functions are orthogonal over the continuous domain [Ref. 10]

$$\int_0^{+\infty} B_n(\kappa) B_m(\kappa) d\kappa = \frac{1}{h_n} \frac{(r_n^c)^2}{r_{n-1} r_n} \delta_{nm} \tag{8}$$

but not over the discrete domain. In the limit when all h_n tend to zero, they satisfy

$$\lim_{\{h_n\} \to 0} \sum_{n=1}^{+\infty} B_n(\kappa) B_n(\kappa') h_n = \delta(\kappa - \kappa') \tag{9}$$

We can therefore call the discrete basis functions 'pseudo-orthonormal' over the discrete domain, in the sense that, in the limit for ever smaller discretisations, they become truly orthogonal.

We use as discrete representation for the modified spectral extinction function

$$B(\kappa) = \frac{\sqrt{\pi}}{2} \frac{1}{\kappa} \sum_{n=1}^{N} c_n B_n(\kappa) \tag{10}$$

It can be shown that, if we take

$$c_n = \frac{h_n}{r_n^c} S(r_n^c) \tag{11}$$

the representation (10) converges to the correct continuous limit (i.e. the integral (3)) when the $\{h_n\}$ tend to zero [Ref. 10]. From (11) it is obvious that our interpolation method also solves the inversion problem. The coefficients $\{c_n\}$ are, up to a factor fixed by the r-axis sampling, values of the underlying surface density distribution.

By substituting the discrete representation (10) in the inversion formula (5), and by integrating over r, we can compute expressions for some integrated distribution quantities (i.e. density quantities), in terms of the coefficients $\{c_n\}$.

For the aerosol total number density we find [Ref. 10]

$$N_{tot} \overset{\Delta}{=} \frac{1}{4\pi} \int_0^{+\infty} \frac{S(r)}{r^2} dr = \frac{1}{4\pi} \sum_{n=1}^{N} c_n \frac{(r_n^c)^2}{r_{n-1} r_n} \tag{12}$$

For the total surface density we get

$$S_{tot} \overset{\Delta}{=} \int_0^{+\infty} S(r) dr = \sum_{n=1}^{N} c_n r_n^c \tag{13}$$

and for the total volume density

$$V_{tot} \overset{\Delta}{=} \frac{1}{3} \int_0^{+\infty} r S(r) dr = \frac{1}{3} \sum_{n=1}^{N} c_n (r_n^c)^2 \tag{14}$$

Up to now, we worked with the modified extinction function $B(\kappa)$, which contains the usually unknown constant $b_\infty = S_{tot}$. From the definition (4a) and by using (10) and (13) we can now write down the discrete representation for the true extinction function $\beta(\kappa)$, as follows

$$\beta(\kappa) = \frac{1}{2} \sum_{n=1}^{N} c_n \left(r_n^c - \frac{\sqrt{\pi}}{2} \frac{1}{\kappa} B_n(\kappa) \right) \tag{15}$$

Expression (15) is the spectral interpolation function used in the numerical implementation.

Finally, we need to determine the coefficients $\{c_n\}$.

Consider given extinction measurements $\{\beta_m,\ 1 \le m \le M\}$ with absolute errors $\{\varepsilon_m,\ 1 \le m \le M\}$ at wavelengths $\{\lambda_m,\ 1 \le m \le M\}$, or equivalently at effective wavenumbers $\{\kappa_m = (n-1)2\pi/\lambda_m,\ 1 \le m \le M\}$. The aim is to determine the coefficients such that the extinction function $\beta(\kappa)$, given by (15), closely passes through the measured data. The most straightorward solution is a least square fit with cost function

$$J_1(\{c_n\}) \stackrel{\Delta}{=} \frac{\sum_{m=1}^{M} w_m(\beta_m - \beta(\kappa_m))^2}{\sum_{m=1}^{M} w_m(\beta_m)^2} \qquad (16)$$

and positive weights $\{w_m,\ 1 \le m \le M\}$, which typically depend on the errors. When this was applied to data with a high degree of uncertainty, it was found necessary to introduce a regularisation of the minimisation problem. This was done by introducing a second cost term, of the form

$$J_2(\{c_n\}) \stackrel{\Delta}{=} \rho^2 \frac{\int_0^{+\infty} \frac{1}{S(r)}\left(\frac{dS(r)}{dr}\right)^2 \frac{dr}{r}}{\int_0^{+\infty} S(r)\frac{dr}{r}} \qquad (17)$$

where ρ is an empirical constant of dimension [μm] and of the order of 0.1. The effect of this term is to reduce the oscillatory behaviour of the coefficients and hence of the resulting surface density distribution. Functional (17) is implemented by discretising the integrals and by relating the discrete values $S(r_n^c)$ to the unknown coefficients, using (11).

The coefficients are then obtained by minimising the total cost function

$$J(\{c_n\}) = aJ_1(\{c_n\}) + bJ_2(\{c_n\}) \qquad (18)$$

with constants a and b, subject to the constraints

$$\beta_m - \varepsilon_m \le \beta(\kappa_m) \le \beta_m + \varepsilon_m,\quad m = 1,\ldots M \qquad (19)$$

and

$$\begin{aligned} &0 \le c_1 < 10^{-6} \\ &0 \le c_n < +\infty,\quad n = 2,\ldots N-1 \\ &0 \le c_N < 10^{-6} \end{aligned} \qquad (20)$$

Constraints (19) assure that the interpolant passes through the error bars of the extinction measurements, while conditions (20) result in a surface density distribution that is positive and zero at the edges of the r-axis discretisation region. The constants a and b are to be fixed by numerical experimenting. We solved the problem (18)-(20) with a Generalized Reduced Gradient Method [Refs. 11-12].

3. NUMERICAL RESULTS

To examine the applicability of the inversion formula (5) and of the interpolation algorithm, numerical tests were done with computer simulated extinction data, using ADA as forward model. In all subsequent examples, aerosol size is measured in μm and densities (concentrations) are expressed per m^3. Test number density distributions were taken to be log-normal

$$N(r) = N_{tot}\frac{1}{\sqrt{4\pi}}\frac{1}{\ln\sigma}\frac{1}{r}e^{-\frac{\ln^2\frac{r}{r_m}}{2\ln^2\sigma}},\quad \int_0^{+\infty} N(r)dr = N_{tot} \qquad (21)$$

A) Inversion by the continuous formula (5).

Consider a bimodal number density, consisting of the sum of two log-normal distributions with parameters r_m=0.7, σ=1.4, amplitude A=0.9 and r_m=3.0, σ=1.3, amplitude A=0.09. We computed the modified extinction function $B(\kappa)$ and then applied the inversion formula (5) to reconstruct the surface density distribution. The integrals were numerically calculated with the trapezium rule. A low pass filter in wavenumber space was used to limit the infinite integration range. This truncation is the main cause of error. Increasing the range of integration and the density of the discretisation of the integrands both reduce the errors, in the forward and inverse calculation. For 10000 wavelength points and 2000 radius points, we get a root mean square (rms) error between the original and reconstructed surface density distributions of 0.9% over a 0.1 – 10.0 μm range. Fig. 1 shows the computed extinction function associated with the bimodal distribution plotted in Fig. 2. This example shows that a straightforward discretisation of the inversion formula can give very good results, provided the extinction function is very densily sampled and the data is exact.

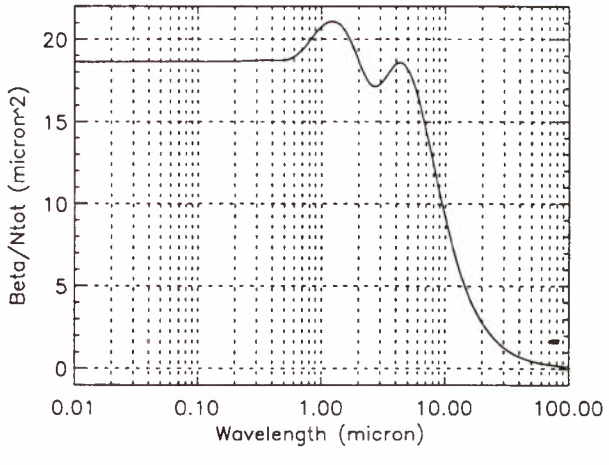

Fig. 1 : Normalized extinction coefficient as function of wavelength, obtained by the ADA for the $S(r)$ in Fig. 2.

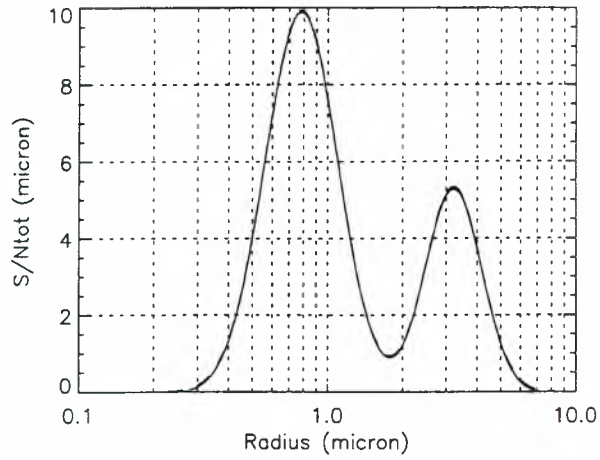

Fig. 2 : Normalized surface density distribution as function of radius. The (invisible) dashed line is the initial distribution, the solid line the reconstruction obtained by (5).

The reason for the necessity of the high number of sample points is the fast oscillatory behaviour of the inverse integrand, when reconstructing the larger radius part of the surface density distribution. Real atmospheric data are not sufficiently densily measured, do not cover a sufficiently large wavelength range and have error bars. For these reasons, a straightforward application of the inversion formula cannnot be used.

B) Results obtained with the discrete algorithm.

The following examples show the behaviour of the algorithm for varying number of measurement points and error bars.

Consider again the bimodal from A. We computed the extinction function $\beta(\kappa)$, sampled it in M=51 points, and reconstructed the original distribution with N=15 basis functions. Reconstructed surface density distributions were interpolated by cubic splines from the N discrete values. Uniformly distributed random noise was added to the extinction samples, giving error bars of a) 3% and b) 10%.

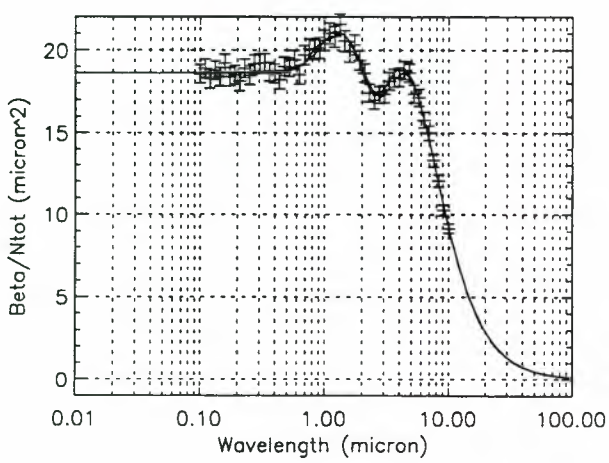

Fig. 3. Initial (dashed) and interpolated (solid) normalized extinction from 51 samples with 3% error.

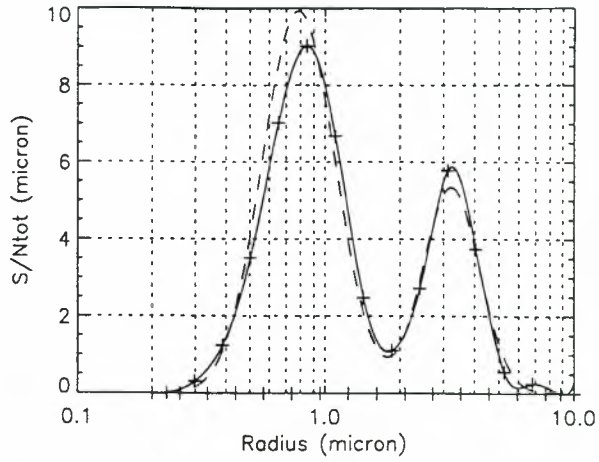

Fig. 4. Initial (dashed) and reconstructed (solid) normalized surface density distribution from 51 samples with 3% error.

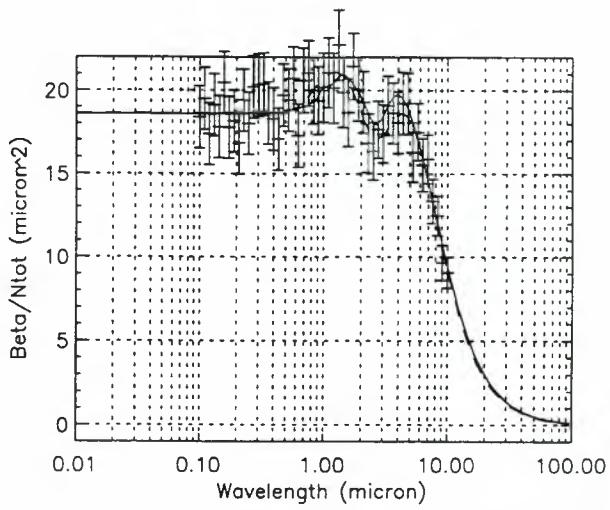

Fig. 5. Initial (dashed) and interpolated (solid) normalized extinction from 51 samples with 10% error.

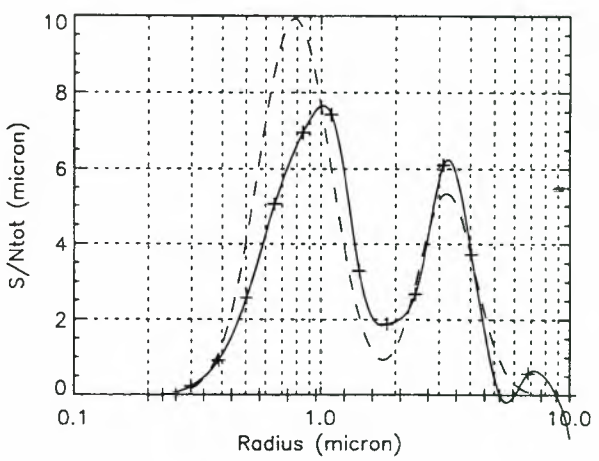

Fig. 6. Initial (dashed) and reconstructed (solid) normalized surface density distribution from 51 samples with 10% error.

Figs. 3 and 5 show the interpolation of the extinction function and Figs. 4 and 6 the surface density distributions. The rms errors are : on the extinction function 0.8% and 2.4% and on the surface density distribution 12.4% and 31.8%, for cases a and b, repectively. The relative errors on the total surface density S_{tot} and total volume density V_{tot} are respectively 0.05% and 1.3% for a and 0.2% and 3.9% for b. This shows that, although the shape of the reconstructed surface density distribution is in error, the integrated quantities are obtained with a smaller error than the error on the original extinction samples. The reason for these good results is that the interpolation algorithm predicts with good accuracy the low wavelength limit of the extinction function, and $S_{tot} = 2 \lim_{\kappa \to +\infty} \beta(\kappa)$.

Fig. 7 shows the interpolation of $\beta(\kappa)$ when $b = 0$ in (18), for error case a. Fig. 8 shows the resulting surface density distribution. It is clear, by comparing Figs. 3, 4 with 7, 8, that the presence of J_2 is necessary to stabilize the inversion. However, J_2 has little effect on the quality of the interpolation (rms error 0.5%). So this means that the surface density distributions of Figs. 4 and 8, although largely different, produce almost the same extinction interpolation curve. This example shows that the inversion problem is much more sensitive to measurement errors than the interpolation problem and one can still have a good interpolation with a bad surface density distribution.

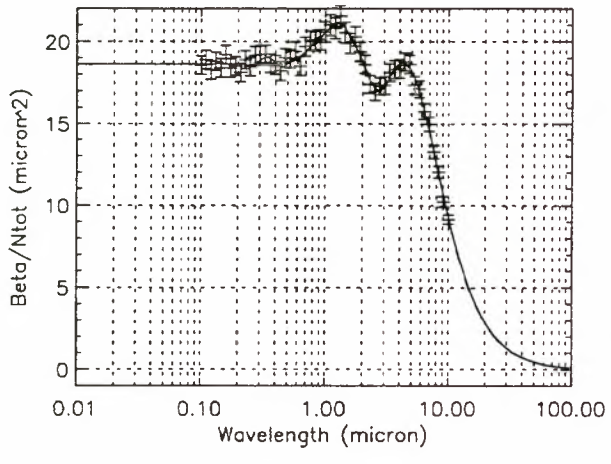

Fig. 7. Initial (dashed) and interpolated (solid) normalized extinction from 51 samples with 3% error, without using the second term in the total cost function (18).

We now consider a single log-normal number density distribution with parameters r_m=1.0, σ=1.35, A=1.0. We use only M=5 extinction samples and again N=15 basis functions, and consider the same relative error bars of a) 3% and b) 10%. Figs. 9 and 11 show the interpolation of the extinction function, while in Figs. 10 and 12 the respective surface density distributions are plotted. The rms errors are : on the extinction function 2.8% and 8.2% and on the surface density distribution 15.0% and 27.5%, for cases a and b repectively. The relative errors on the total surface density S_{tot} and total volume density V_{tot} are respectively 0.6% and 1.6% for a and 2.6% and 8.0% for b.

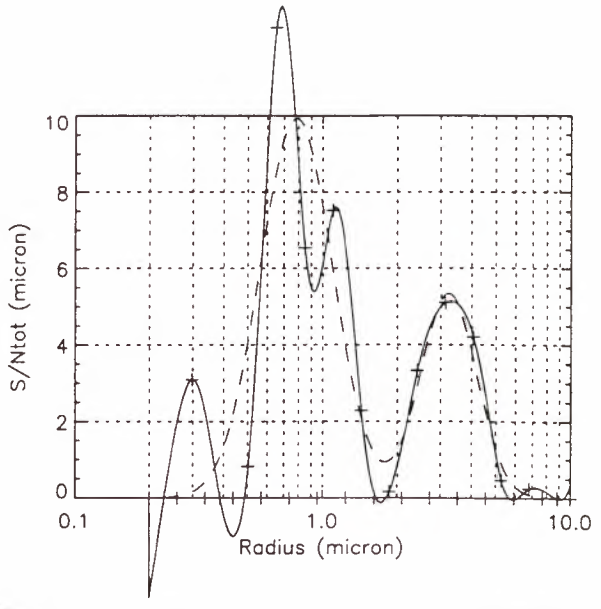

Fig. 8. Initial (dashed) and reconstructed (solid) normalized surface density distribution associated with Fig. 7.

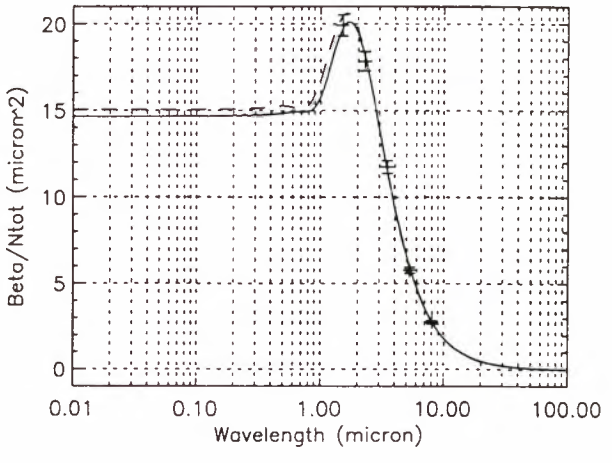

Fig. 9. Initial (dashed) and interpolated (solid) normalized extinction from 5 samples with 3% error.

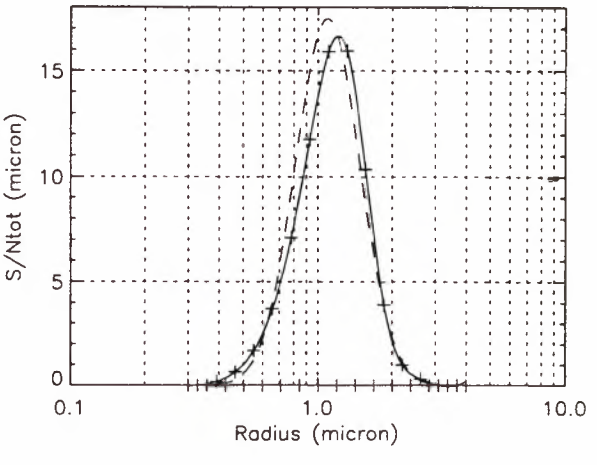

Fig. 10. Initial (dashed) and reconstructed (solid) normalized surface density distribution from 5 samples with 3% error.

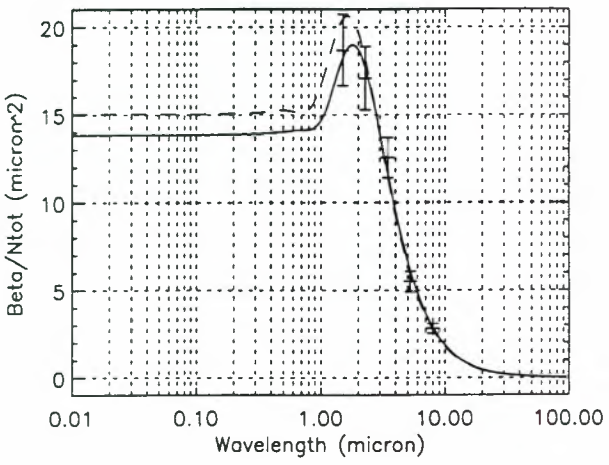

Fig. 11. Initial (dashed) and interpolated (solid) normalized extinction from 5 samples with 10% error.

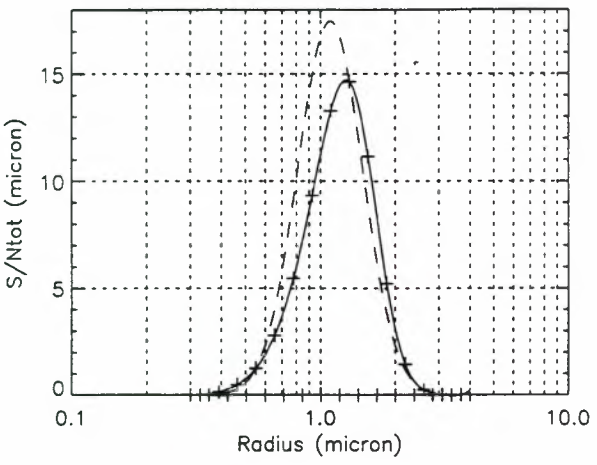

Fig. 12. Initial (dashed) and reconstructed (solid) normalized surface density distribution from 5 samples with 10% error.

Figs. 9-12 are to be compared with Figs. 13 and 14, which show the interpolation and inversion for the same case, but now with exact samples. This shows that the algorithm is very powerful in reconstructing the extinction and surface density distribution from very few points, provided the data is accurate, at least for single mode log-normal distributions. We now obtain a rms error on the extinction function of 0.5% and 7.2% on the distribution. The relative error on the total surface density is 0.06% and on the total volume density 0.4%. In this example, the algorithm extrapolates the extinction into the UV region very well, from data that was only available in the IR region.

4. CONCLUSIONS

Numerical tests demonstrated the usefulness of the proposed algorithm for spectral extinction interpolation. Examples for a single and bimodal distribution show that our method is stable when applied to noise-corrupted data. It is capable of reconstructing $\beta(\kappa)$ with a relative rms error that is smaller than the relative error on the initial extinction samples, even when only very few data points are available. For example, interpolating from 5 samples, having a 10 % relative error, in the case of a single log-normal number density distribution, results in an interpolation error of about 8% rms over the whole spectrum. The method produces, as by-product, the underlying size distribution (number, surface and volume density distributions), to a reasonable degree of accuracy. The relative error on the inversion is about 3 to 4 times higher than that on the samples, for single and bimodal log-normal number density distributions. But integrated quantities, such as total surface and volume densities, are retrieved to a much higher accuracy. For the case already mentioned above, total surface and volume density were retrieved to within 0.6% and 1.6%, repectively. In general, it was found that the inverse problem was much more sensitive to noise, than the interpolation problem.

More work is planned to further improve the algorithm. In particular, the choice of the functional (17) needs to be examined in more detail.

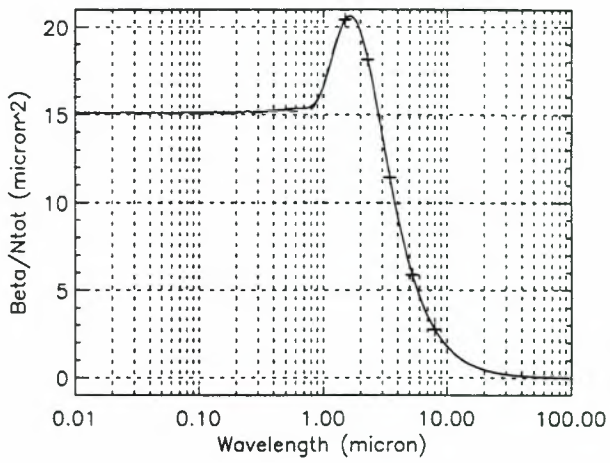

Fig. 13. Initial (dashed) and interpolated (solid) normalized extinction from 5 exact samples.

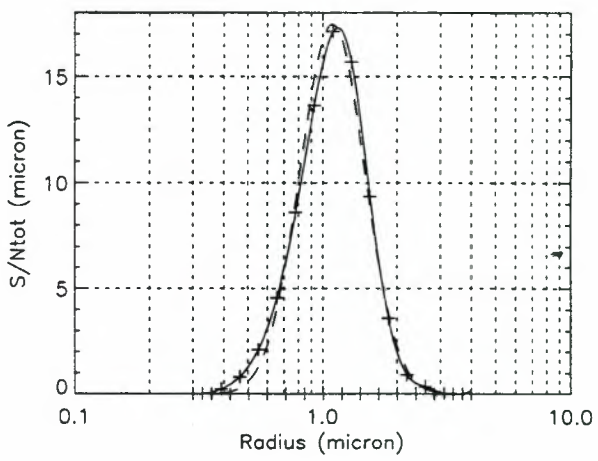

Fig. 14. Initial (dashed) and reconstructed (solid) normalized surface density distribution from 5 exact samples.

5. ACKNOWLEDGEMENT

This research was funded by the European Space Agency in the framework of the Data User Programme (http://styx.esrin.esa.it:8099/), contract AMASDU (Aerosol Mapping Algorithms for Satellite Data Users, contract no. 12526/97/I-HE).

6. REFERENCES

1. Box G. P., Box M. A. and Krücker J., 1996, Information content and wavelength selection for multispectral radiometers, *J. Geophys. Res.*, 101, 19211-19214.

2. Lambert, A., Grainger R. G., Rogers H. L., Norton W. A., Rodgers C. D. and Taylor F. W., 1996, The H_2SO_4 Component of stratospheric aerosols derived from satellite infrared extinction measurements: Application to stratospheric transport studies, *Geophys. Res. Lett.*, 23, 2219-2222.

3. Twomey S., 1975, Comparison of constrained linear inversion and an iterative non-linear algorithm applied to the indirect estimation of particle size distributions, *J. Comput. Phys.*, 18, 188-200.

4. Smith C. B., 1982, Inversion of the anomalous diffraction approximation for variable complex index of refraction near unity, *Applied Optics*, 21, 3363-3366.

5. Klett J. D., 1984, Anomalous diffraction model for inversion of multispectral extinction data including absorption effects, *Applied Optics*, 23, 4499-4508.

6. Wang J. and Hallett, F. R., 1996, Spherical particle size determination by analytical inversion of the UV-visible-NIR extinction spectrum, *Applied Optics*, 35, 193-197.

7. Amato U., Di Bello D., Esposito F., Serio C., Pavese G. and Romano F., 1996, Intercomparing the Twomey method with a multimodal lognormal approach to retrieve the aerosol size distribution, *J. Geophys. Res.*, 101, 19267-19275.

8. Thomason L. W., Poole L. R. and Deshler T., 1997, A global climatology of stratospheric aerosol surface area density deduced from SAGE II measurements: 1984-1994, *J. Geophys. Res.*, 102, 8967-8976.

9. van de Hulst H. C., 1981, Light scattering by small particles, *Dover Publications Inc.*, New York.

10. Franssens G., 1999, Determination of particle size distributions from extinction data based on the anomalous diffraction approximation, pre-print.

11. Lasdon L. S., Waren A. D., Jain A. and Ratner M., 1978, Design and Testing of a Generalized Reduced Gradient Code for Nonlinear Programming, *ACM Trans. on Math. Software*, 4, 1, 34-50.

12. Lasdon L. S. and Waren A. D., 1979, Generalized Reduced Gradient Software for Linearly and Nonlinearly Constrained Problems, in *"Design and Implementation of Optimization Software"*, Greenberg H., ed., Sijthoff and Noordhoff, pubs.